A Two-Step Semiglobal Filtering Approach to Extract DTM From Middle Resolution DSM

4 authors:

Zhang Yanfeng
Wuhan University
7 PUBLICATIONS   **2** CITATIONS

SEE PROFILE

Yongjun Zhang
Wuhan University
112 PUBLICATIONS   **665** CITATIONS

SEE PROFILE

Yunjun Zhang
University of Miami
5 PUBLICATIONS   **9** CITATIONS

SEE PROFILE

Zongze Zhao
Henan Polytechnic University
5 PUBLICATIONS   **14** CITATIONS

SEE PROFILE

Some of the authors of this publication are also working on these related projects:

Dense Image Matching for Digital Surface Model Generation View project

Las Class View project

A Two-Step Semiglobal Filtering Approach to Extract DTM From Middle Resolution DSM

Yanfeng Zhang, Yongjun Zhang, Zhang Yunjun, and Zongze Zhao

Abstract—Many filtering algorithms have been developed to extract the digital terrain model (DTM) from dense urban light detection and ranging data or the high-resolution digital surface model (DSM), assuming a smooth variation of topographic relief. However, this assumption breaks for a middle-resolution DSM because of the diminished distinction between steep terrains and nonground points. This letter introduces a two-step semiglobal filtering (TSGF) workflow to separate those two components. The first SGF step uses the digital elevation model of the Shuttle Radar Topography Mission to obtain a flat-terrain mask for the input DSM; then, a segmentation-constrained SGF is used to remove the nonground points within the flat-terrain mask while maintaining the shape of the terrain. Experiments are conducted using DSMs generated from Chinese ZY3 satellite imageries, verified the effectiveness of the proposed method. Compared with the conventional progressive morphological filter method, the usage of flat-terrain mask reduced the average root-mean-square error of DTM from 9.76 to 4.03 m, which is further reduced to 2.42 m by the proposed TSGF method.

Index Terms—Digital surface model (DSM), digital terrain model (DTM), middle resolution, semi-global filtering (SGF), Shuttle Radar Topography Mission (SRTM).

I. INTRODUCTION

A. Background

DIGITAL terrain models (DTMs) provide an important source of data that can be used in many applications, such as terrain analysis [1]–[3] and the generation of digital ortho maps. Light detection and ranging (LiDAR) and digital surface models (DSMs) are two fundamental data sources for DTM extraction. DTMs represent terrain surfaces, while LiDAR or DSMs consist of both terrain and objects on the terrain surface, which correspond to ground points and nonground points, respectively. In order to obtain a DTM, the nonground points need to be identified and removed from LiDAR or DSM, which is called the filtering process [4].

Many filtering algorithms have been proposed for DTM extraction, such as mathematical morphological

methods [5], [6] (a typical mathematical morphological algorithm will be used for comparative experiments in this letter), triangulated irregular network-based methods [7], [8], slope-based methods [9], [10], and scanline-based methods [11]. These filtering algorithms usually assume that the elevation variation of topographic relief is smooth, while the variation of nonground points is abrupt. The above assumption is usually true for LiDAR since its measurement density is high enough to have at least one point per square meter (measurement density is substantially equal to resolution, and its effect on DTM extraction will be further introduced in the following paragraph), and it is likely to be limited to a subset of geographical areas, such as urban areas which have few steep terrains. As a result, most of the state-of-the-art algorithms can effectively extract a DTM from LiDAR data, and similar in the case of high spatial resolution DSM.

However, the above filtering methods are not suitable for filtering middle-resolution DSMs, which are still widely used, with a lot of middle-resolution stereo satellite imagery (such as ZY-3, TH-1, Cartosat-1, and SPOT 5/6). These DSMs usually have: 1) a resolution lower than 3 m and 2) a large-scale cover of over 2000 km^2. Both of the two characteristics make it difficult to remove the nonground points while keeping the shape of steep terrains. First regarding the resolution, elevation variations caused by nonground points are smoother in lower-resolution DSM, which makes the elevation variations caused by nonground points in middle-resolution DSM indistinguishable from the variations caused by abrupt topographic relief. The significant effect of reduced resolution on DTM extraction has been recognized years ago but scarcely studied [4], [12]. Second, such a large-scale DSM tends to contain steep mountainous terrain, which also hampers the assumption that the elevation variation of topographic relief is smooth while the variation in nonground points is abrupt. In summary, the basic assumption for LiDAR filtering methods is not suitable any more for middle-resolution DSM; thus, it is prone to damage steep terrains when filtering algorithms remove nonground points in flat-terrain areas. Chen *et al.* [13] presented a method to handle with steep mountainous areas, but it was designed for high-resolution DTM generation from highly dense point clouds (6 points/m^2). Another method [12] was aimed at solving this problem by improving the resolution of DSM in order to hold the assumption. However, multi-source DSMs were needed, which led to the limitation of the practicability.

B. Proposed Approach

For a middle-resolution DSM, it is mainly the flat-terrain areas, more specifically the built-up areas, that need to be

This article has been accepted for inclusion in a future issue of this journal. Content is final as presented, with the exception of pagination.
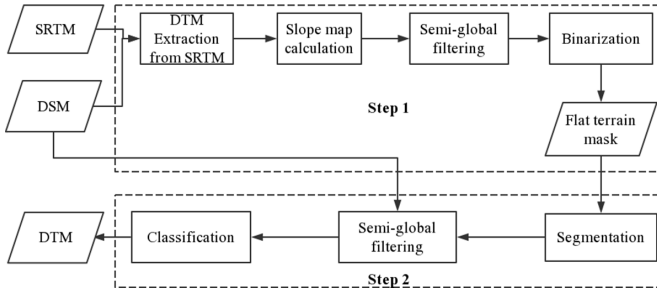
2

IEEE GEOSCIENCE AND REMOTE SENSING LETTERS

Fig. 1.   Flowchart of the proposed TSGF method.

processed. It is also important to take some strategies to keep the mountainous terrains from being damaged. Therefore, we think the DTM extraction process can be divided into two steps: 1) detect the flat-terrain mask of the DSM and 2) remove the nonground points in the flat-terrain areas. The two-step method separates the flat terrains from steep mountainous terrains, thus making nonground points in the flat-terrain areas distinguishable from terrains.

Based on the above analysis, we propose the two-step semiglobal filtering (TSGF) method, which is presented in the following sections. Section II describes the methodology of the two-step workflow. Section III shows the experimental results. A brief discussion is illuminated in Section IV with our conclusion in Section V.

C. Related Work

The SGF algorithm is first proposed to extract the DTM from a LiDAR data set [14]. The energy function employed a locally calculated balance coefficient which was designed for highly dense point clouds, but not suitable for the low-resolution DSM filtering. This letter is based on our previous work [15], in which the flat-terrain mask was detected with the input DSM; however, it tended to fail in areas with high building density. To solve this problem, in this work, the input DSM is replaced with Shuttle Radar Topography Mission (SRTM) [16] data to detect the flat-terrain mask. Moreover, the energy function for DSM filtering is improved to achieve a superior DTM. In addition, more experiments including quality evaluation and quantitative assessment are conducted in order to verify the effectiveness of TSGF.

II. METHOD

As presented in Fig. 1, the proposed method consists of two steps: 1) detecting flat-terrain areas and 2) filtering the flat terrains. For the first step, a low-resolution DTM geographically corresponding to the input DSM is extracted from the SRTM, and then a slope map of the DTM is computed and processed by SGF. After that, the filtered slope map is binarized to achieve a flat-terrain mask, which is mapped back on the input DSM and segmented. For the second step, SGF is employed to process the DSM with the constraint of segmentation and obtain a classification surface, which is then used to remove the nonground points from the input DSM. The final DTM is generated by the interpolation of the ground points.

A. Semiglobal Filtering of Slope Map

Slope is one of the most important DSM characteristics, which can be used to distinguish steep terrains from

flat terrains. However, terrain type cannot directly be determined by slope because a pixel at flat terrain does not always have a lower slope than a pixel at mountainous terrain.

Nevertheless, most of pixels at flat terrain have a lower slope than those at mountainous terrain. A nonlocal filter keeps the slope changing smoothly on the whole DSM, and thus would enhance the slope difference between flat terrain and mountainous terrain by suppressing high slope at flat-terrain area while promoting low slope at mountainous-terrain area.

The nonlocal filtering of a slope map assigns new slope values to each pixel. The new slope should be as close as possible to the original slope with the constraint that changes in the neighbor slopes must be as small as possible. Since the slopes used in the nonlocal filtering are discrete values while the initial slope map is continuous, it should be discretized before filtering. In this letter, the slope is discretized by one degree; therefore, the discretized slope map has 90 levels. Filtering of the slope map can be modeled as a labeling problem with the following energy function which depends on slope map S:

$$E(S) = \sum_p \left(C(p, S_p) + \sum_{q \in N_p} P_1 T[|S_p - S_q| = 1] \right.$$
$$\left. + \sum_{q \in N_p} P_2 T[|S_p - S_q| > 1] \right)$$
$$T[x] = \begin{cases} 1, & x = \text{true} \\ 0, & x = \text{false} \end{cases}$$
$$C(p, S_p) = |S_p - S'_p|/90 \tag{1}$$

where S_p represents the possible slope level of p, S'_p represents the original slope level of p, and P_1 and P_2 are constants, which are the penalties for slope level changes. q is the neighbor pixel of p.

The optimization of (1) is the minimization of whole energy, which is achieved by assigning proper slope to each point. The energy function can be solved with semiglobal optimization, which was originally used in stereo matching [17]. The algorithm aggregates the cost for each point from eight directions independently, and the optimal label of each point is obtained by the "winner takes all" principle. The label in the original algorithm was disparity, which is replaced in this letter with a slope value.

B. Generation of Flat-Terrain Mask Based on SRTM

The method for the generation of flat-terrain mask is as follows. First, a DTM is extracted from the SRTM corresponding to the spatial coverage of input DSM, which is then used to generate a slope map for producing an initial flat-terrain mask by SGF (Section II-A) and binarization. Finally, the initial flat-terrain mask is refined and mapped back on the input DSM, thus achieving the final flat-terrain mask of the input DSM. Modified from our previous work [15], we use SRTM in this letter, which is basically a low-resolution DTM without nonground points, rather than DSM itself to detect the flat terrain. This gives a better estimation of nonground point mask for a low-resolution DTM.
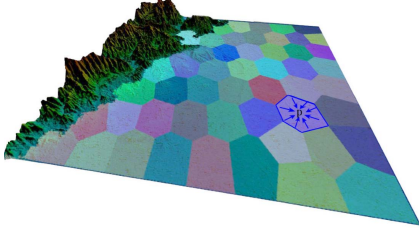
This article has been accepted for inclusion in a future issue of this journal. Content is final as presented, with the exception of pagination.

ZHANG *et al.*: TSGF APPROACH TO EXTRACT DTM

3

Fig. 2.   Segmentation-constrained SGF.

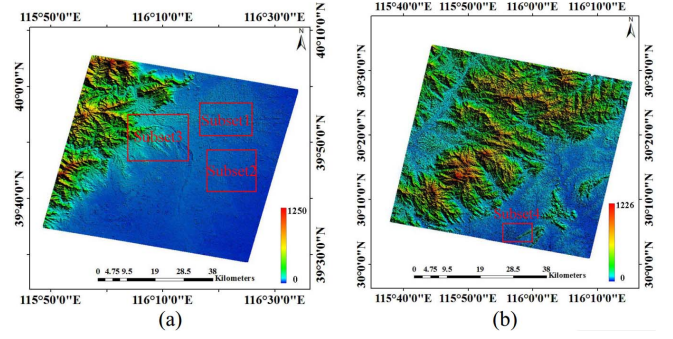(a)   (b)

Fig. 3.   Overview of experimental data. (a) "Beijing" DSM with a resolution of 10 m, which was located in Beijing. (b) "Huanggang" DSM with a resolution of 5 m, which was located in Huanggang. Four typical subsets are presented in red color and also shown in Fig. 4.

In detail, the binarization threshold used in this letter is 4°. Besides, a region growing-based segmentation method is used and the patches below 100 pixels are removed since binarization may generate small patches in the mask. The two thresholds are both empirically adopted, and they are suggested for processing DSMs with a resolution of 5–10 m.

C. Segmentation-Constrained Semiglobal Filtering of DSM

Within a flat-terrain mask, it becomes possible to distinguish ground points from nonground points because the topographic relief is smooth while the elevation variation caused by nonground points is abrupt. In particular, the flat-terrain mask is first divided into segments, and SGF is implemented within each segment independently. Fig. 2 shows the segmentation-constrained SGF of a DSM. The segmentation algorithm used is the simple linear iterative clustering algorithm [18], and the super-pixel step size for segmentation is 100 in this letter.

The filtering of a DSM can also be modeled as a labeling problem, in which the label corresponds to the height level. The energy function for SGF of a DSM is as follows:

$$E(H) = \sum_p \left(\begin{array}{l} \gamma_p C(p, H_p) \\ + (1 - \gamma_p) \left(\sum_{q \in N_p} P_3 T[|H_p - H_q| = 1] \right. \\ \left. + \sum_{q \in N_p} P_4 T[|H_p - H_q| > 1] \right) \end{array} \right)$$

(2)

$$\gamma_{p \in S(i)} = \beta \exp \left(-\frac{H_p' - H_{\min}(i)}{H_{\max}(i) - H_{\min}(i)} \right)$$

(3)

$$C(p, H_p) = \begin{cases} 1 - \exp(-\alpha(H_p - H_{\min}'(p))), & \text{if } H_p \le H_p' \\ \infty, & \text{if } H_p > H_p' \end{cases}$$

(4)

where γ_p is the balance coefficient, which is calculated with an original height level H_p'. H_p is the possible height level. $S(i)$ is the ith segment. $H_{\max}(i)$ and $H_{\min}(i)$ are the maximum and minimum height values within the segment $S(i)$. $H_{\min}'(p)$ is the minimum height level within the local window of point p. The window size is 3×3 in this letter. α and β are preset constants. P_3 and P_4 are constants, which are the penalties for height level changes.

It can be seen that the data term $C(p, H_p)$ is truncated at the original height level because the classification surface cannot be higher than the input DSM. The balance coefficient γ_p is used to attract lower height and reject higher height because the nonground points tend to be higher than the surrounding ground points. The balance coefficient is calculated within the segment and thus cannot be affected by the size of the whole mask.

The energy function can also be solved by semiglobal optimization as described in Section II-A; thus, a classification surface is achieved.

D. Classification and DTM Generation

The classification method calculates the elevation change of each point between the classification surface and the original DSM, and if the change is larger than the height-level spacing, the point is classified as a nonground point and removed from the original DSM. Finally, the DTM is generated from the ground points with the inverse distance-weighted interpolation algorithm [19].

III. EXPERIMENT

A. Data

DSMs generated with Chinese ZY-3 imageries were used as the experimental data in this letter. The experimental areas were located at the Beijing and Huanggang of China, which contain mountainous terrains with both abrupt and smooth topographic relief and flat terrains with a large number of urban buildings (Fig. 3). The results of four typical subsets (Fig. 4) are presented in order to obtain more details about DSMs and DTMs. Because ground truth (GT) data were unavailable, manually edited DTMs were used as the GT in order to conduct the quantitative assessment. The manually edited DTMs were carefully acquired by an experienced operator with the guidance of the original stereo imageries.

B. Method

Progressive morphological filtering (PMF) [5] is a typical and frequently used method for automatic extraction of DTMs from LiDAR data sets, which was used in this letter for comparison with the proposed method. To demonstrate the significant influence of flat-terrain mask on the final DTM, we implemented a modified version of PMF method, which performed PMF within the flat-terrain mask to extract a DTM, indicated as PMF + Mask in the following context. The flat-terrain mask used in PMF + Mask is the same as the one used in TSGF.
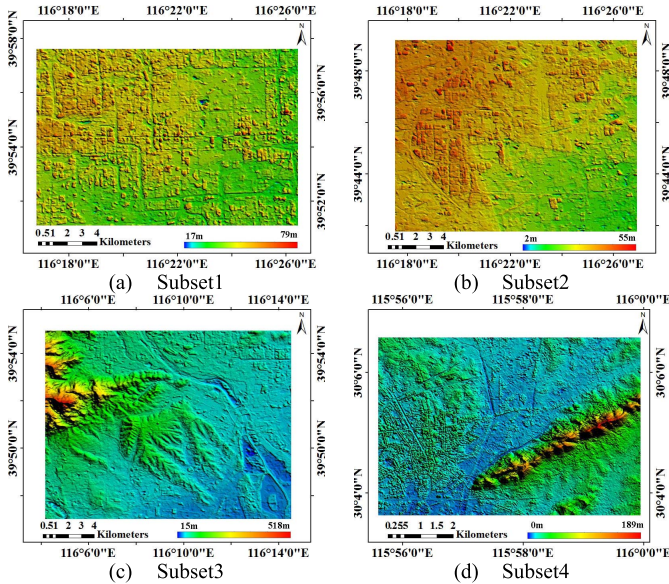
This article has been accepted for inclusion in a future issue of this journal. Content is final as presented, with the exception of pagination.

4   IEEE GEOSCIENCE AND REMOTE SENSING LETTERS

Fig. 4. Overview of four typical subsets picked from the input DSMs. (a)–(c) Subsets picked from the "Beijing" DSM. (d) Subset picked from the "Huanggang" DSM. In particular, (a) and (b) represent the flat-terrain areas whereas (c) and (d) represent the complicated terrain areas which contained both steep mountainous terrains and flat terrains with buildings.

We first conducted visual comparison of the results of the four typical subsets (Section III-C). Then we conducted quantitative assessment (Section III-D), which consists of two parts. For the first part, we evaluated the accuracy of identifying nonground points of the three comparative methods. We obtained the GT of nonground points by comparing the GT with DSMs. Then, three kinds of errors [4], namely, Type I errors (omission errors), Type II errors (commission errors), and total errors were evaluated. For the second part, the residual errors between GT and DTMs processed with PMF, PMF + Mask, and TSGF were collected. Based on the residual errors, the following two indicators were used to evaluate the accuracy: 1) root-mean-square error (RMSE) and 2) mean error (ME).

The TSGF algorithm with C++ language was applied.[1] All the experiments were conducted on a single i7 CPU core. The parameters recommended for TSGF in practice were as follows: $P_1 = 0.1$, $P_2 = 0.3$, $P_3 = 0.3$, $P_4 = 6$, $\alpha = 0.1$, and $\beta = 0.5$. The parameters used for PMF are as follows [5]: $k = 10$, $s = 0.1$, $dh_0 = 2.0$, and $dh_{max} = 3.0$. Using above parameters, both algorithms achieved their best overall performance for the testing sites in this letter.

C. Visual Comparison of DTM

In Fig. 5, the first and second rows show that all of the three methods removed most of the nonground points in flat-terrain areas. However, the third and fourth rows show that PMF heavily damaged the mountainous terrains while PMF + Mask performed much better than PMF since the mountainous terrains were majorly kept. It can also be seen from the third row that PMF + Mask damaged some gentle mountainous terrains, which were robustly kept by TSGF.

[1]The main code of TSGF along with testing data can be found on GitHub: https://github.com/zenmemeinuanqi/Two-step-Semi-Global-Filtering.
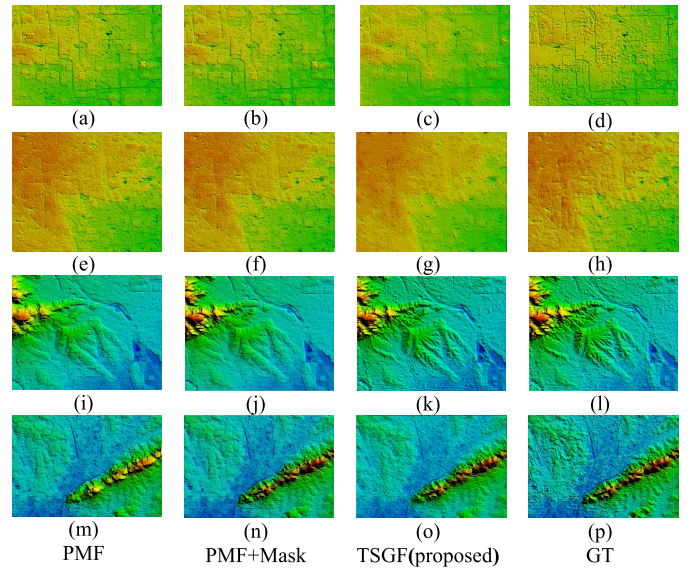

Fig. 5. Visual comparison of the DTMs at different terrains. The columns from left to right display the DTMs processed with (a), (e), (i), and (m) PMF, (b), (f), (j), and (n) PMF + Mask, c), (g), (k), and (o) proposed TSGF, and (d), (h), (l), and (p) GT, respectively.

TABLE I
THREE TYPES OF ERRORS OF PMF, PMF + Mask, AND TSGF
FOR THE FOUR TESTING SUBSETS (%)

		PMF	PMF+Mask	TSGF
Subset1	Type I	**10.68**	**10.68**	18.06
	Type II	22.01	22.01	**8.26**
	Total	18.29	18.29	**11.48**
Subset2	Type I	20.92	20.92	**19.56**
	Type II	11.91	11.91	**7.82**
	Total	14.31	14.31	**10.96**
Subset3	Type I	16.02	**14.23**	29.49
	Type II	31.81	29.38	**8.17**
	Total	30.25	27.88	**10.28**
Subset4	Type I	3.75	**2.65**	8.33
	Type II	30.09	27.51	**5.75**
	Total	27.82	25.36	**5.97**

D. Quantitative Assessment of DTM

As shown in Table I, the results of PMF and PMF + Mask for Subset1 and Subset2 were the same. Regarding Subset3 and Subset4, all the three types of errors of PMF + Mask were less than PMF. And TSGF achieved the best performance among the three comparative methods for all the four testing subsets in terms of Type II errors and total errors. The average total errors of testing subsets for PMF, PMF + Mask, and TSGF were 22.67%, 21.46%, and 9.67%, respectively. Fig. 6 shows the accuracy of DTMs generated by PMF, PMF + Mask, and TSGF. The results of PMF and PMF + Mask for Subset1 and Subset2 were the same. The usage of a flat-terrain mask reduced the average RMSE of PMF from 9.76 to 4.03 m, which is further reduced to 2.42 m by the proposed TSGF method.

IV. DISCUSSION

The results shown in Fig. 5 clearly demonstrate that the extracted DTMs benefited from the usage of flat-terrain mask and the proposed TSGF performed better than PMF.

ME	Subset1	Subset2	Subset3	Subset4
PMF	-1.30	-0.55	-4.83	-9.00
PMF+Mask	-1.30	-0.55	-3.03	-2.93
TSGF	0.17	-0.06	-1.39	-0.72

(a)

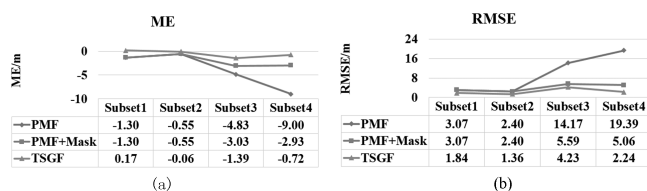| RMSE	Subset1	Subset2	Subset3	Subset4
PMF	3.07	2.40	14.17	19.39
PMF+Mask	3.07	2.40	5.59	5.06
TSGF	1.84	1.36	4.23	2.24

(b)

Fig. 6. (a) RMSEs and (b) MEs of DTMs generated by PMF, PMF + Mask, and the proposed TSGF for the four testing subsets.

In Table I and Fig. 6, the results of PMF and PMF + Mask for Subset1 and Subset2 were the same because the whole subsets were detected as flat terrains. It is noteworthy that the capability of keeping terrains enables TSGF reduces Type II errors significantly at the cost of having a larger Type I errors because some nonground points at steep terrains might be identified as a ground point mistakenly. Nevertheless, according to results in Sections III-C and III-D, the usage of flat-terrain mask was effective to extract a superior DTM. Moreover, TSGF achieved the best accuracy among the three comparative methods for all the testing subsets. It suggests that the proposed energy function for the segmentation-constrained SGF is effective and practical to extract DTM from a middle-resolution DSM.

TSGF has limitations. It removes the nonground points in the flat-terrain areas while keeping steep terrains unchanged. However, there might be large forests in the steep mountainous areas. In that scenario, TSGF will not be able to detect and remove them. This has been an unsolved problem for lots of state-of-the-art methods to extract a DTM from DSM produced by imageries because the forest areas of such a DSM usually have no visible ground points [13], [20].

V. Conclusion

Most of existing filtering methods are designed for dense point cloud and cannot extract DTM from a middle-resolution DSM. To address this issue, we proposed a TSGF method. Experiments carried out on the DSMs produced with ZY-3 satellite images demonstrated the effectiveness of the proposed method. It has three contributions. First, the proposed method includes a practical "two-step" workflow for extracting DTM from a middle-resolution DSM. Second, the proposed method employs SRTM to detect a flat-terrain mask, which can robustly distinguish between steep terrains and flat terrains. Third, the proposed approach includes a new segmentation-constrained SGF method to remove nonground points while maintaining the shape of the terrains. The proposed method would be a helpful tool and has the potential to replace manual editing in DTM production from the middle-resolution DSM. The flat-terrain mask was shown to be very important for the proposed method because DSM filtering could be implemented only within the mask. However, this strong constraint for DSM filtering that may not be robust enough, which is an important facet of the proposed method. Therefore, how to use the mask in a more robust way is worthy of further study.

References

[1] S. A. White and Y. Wang, "Utilizing DEMs derived from LiDAR data to analyze morphologic change in the North Carolina coastline," *Remote Sens. Environ.*, vol. 85, no. 1, pp. 39–47, 2003.
[2] T. R. Martha, N. Kerle, V. Jetten, C. J. van Westen, and K. V. Kumar, "Landslide volumetric analysis using Cartosat-1-derived DEMs," *IEEE Geosci. Remote Sens. Lett.*, vol. 7, no. 3, pp. 582–586, Jul. 2010.
[3] Z. Zhan and B. Lai, "A novel DSM filtering algorithm for landslide monitoring based on multiconstraints," *IEEE J. Sel. Topics Appl. Earth Observ.*, vol. 8, no. 1, pp. 324–331, Jan. 2015.
[4] G. Sithole and G. Vosselman, "Experimental comparison of filter algorithms for bare-Earth extraction from airborne laser scanning point clouds," *ISPRS J. Photogramm. Remote Sens.*, vol. 59, nos. 1–2, pp. 85–101, 2004.
[5] K. Zhang, S.-C. Chen, D. Whitman, M.-L. Shyu, J. Yan, and C. Zhang, "A progressive morphological filter for removing nonground measurements from airborne LIDAR data," *IEEE Trans. Geosci. Remote Sens.*, vol. 41, no. 4, pp. 872–882, Apr. 2003.
[6] C. Geiß, M. Wurm, M. Breunig, A. Felbier, and H. Taubenböck, "Normalization of TanDEM-X DSM data in urban environments with morphological filters," *IEEE Trans. Geosci. Remote Sens.*, vol. 53, no. 8, pp. 4348–4361, Aug. 2015.
[7] P. Axelsson, "DEM generation from laser scanner data using adaptive TIN models," *Int. Arch. Photogramm. Remote Sens.*, vol. 33, no. 1, pp. 110–117, 2000.
[8] X. Zhao, Q. Guo, Y. Su, and B. Xue, "Improved progressive TIN densification filtering algorithm for airborne LiDAR data in forested areas," *ISPRS J. Photogramm. Remote Sens.*, vol. 117, pp. 79–91, Jul. 2016.
[9] G. Vosselman, "Slope based filtering of laser altimetry data," *Int. Arch. Photogramm. Remote Sens.*, vol. 33, pp. 935–942, Jul. 2000.
[10] M. Debella-Gilo, "Bare-earth extraction and DTM generation from photogrammetric point clouds including the use of an existing lower-resolution DTM," *Int. J. Remote Sens.*, vol. 37, no. 13, pp. 3104–3124, 2015.
[11] X. Meng, L. Wang, J. L. Silván-Cárdenas, and N. Currit, "A multi-directional ground filtering algorithm for airborne LiDAR," *ISPRS J. Photogram. Remote Sens.*, vol. 64, no. 1, pp. 117–124, 2009.
[12] M. Sreedhar, S. Muralikrishnan, and V. K. Dadhwal, "Automatic conversion of DSM to DTM by classification techniques using multi-date stereo data from Cartosat-1," *J. Indian Soc. Remote Sens.*, vol. 43, no. 3, pp. 513–520, 2015.
[13] Q. Chen, H. Wang, H. Zhang, M. Sun, and X. Liu, "A point cloud filtering approach to generating DTMs for steep mountainous areas and adjacent residential areas," *Remote Sens.*, vol. 8, no. 1, pp. 71–93, 2016.
[14] X. Hu, L. Ye, S. Pang, and J. Shan, "Semi-global filtering of airborne LiDAR data for fast extraction of digital terrain models," *Remote Sens.*, vol. 7, no. 8, pp. 10996–11015, 2015.
[15] Y. Zhang, Y. Zhang, Y. Zhang, and X. Li, "Automatic extraction of DTM from low resolution DSM by two-steps semi-global filtering," *ISPRS Ann. Photogramm. Remote Sens. Spatial Inf. Sci.*, vol. III-3, no. 3, pp. 249–255, 2016.
[16] J. J. Becker *et al.*, "Global bathymetry and elevation data at 30 arc seconds resolution: SRTM30_PLUS," *Marine Geodesy*, vol. 32, no. 4, pp. 355–371, 2009.
[17] H. Hirschmüller, "Stereo processing by semiglobal matching and mutual information," *IEEE Trans. Pattern Anal. Mach. Intell.*, vol. 30, no. 2, pp. 328–341, Feb. 2008.
[18] R. Achanta, A. Shaji, K. Smith, A. Lucchi, P. Fua, and S. Süsstrunk, "SLIC superpixels compared to state-of-the-art superpixel methods," *IEEE Trans. Pattern Anal. Mach. Intell.*, vol. 34, no. 11, pp. 2274–2282, Nov. 2012.
[19] C. Childs, "Interpolating surfaces in ArcGIS spatial analyst," *ArcUser*, vol. 7, no. 3, pp. 32–35, 2004.
[20] R. Perko, H. Raggam, K. H. Gutjahr, and M. Schardt, "Advanced DTM generation from very high resolution satellite stereo images," *ISPRS Ann. Photogramm. Remote Sens. Spatial Inf. Sci.*, vol. II-3, no. W4, pp. 165–172, 2015.